An iterative scheme for the 2D ANNNI model



1987 J. Phys. A: Math. Gen. 20 471

(http://iopscience.iop.org/0305-4470/20/2/032)

J. Phys. A: Math. Gen. **20** (1987) 471-480. Printed in the UK

# An iterative scheme for the 2D ANNNI model

M A S Saqi† and D S McKenzie

Department of Physics, King's College London, The Strand, London WC2R 2LS, UK

Received 21 April 1986, in final form 28 May 1986

**Abstract.** The 2D ANNNI model is studied using a new iterative method, the method of ring recurrence. We show that the method produces an iterative scheme which enables the phase diagram and behaviour of the wavevector to be obtained using low-order matrices, with minimal computational effort. We find a one-dimensional attractor associated with the incommensurate phase.

## 1. Introduction

The axial next-nearest-neighbour Ising (ANNNI) model (Elliot 1961) is one of the simplest statistical mechanical models to show complex modulated phases. The two-dimensional model is defined in figure 1, where nearest-neighbour couplings are labelled

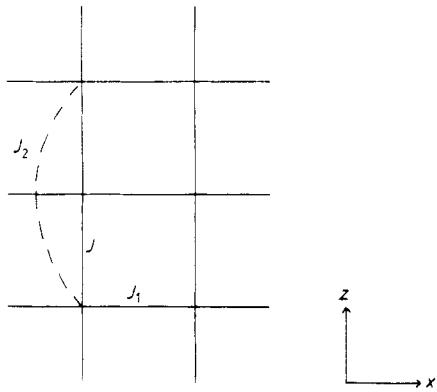


**Figure 1.** The 2D ANNNI model. $J$ and $J_1$ are ferromagnetic nearest-neighbour couplings; $J_2$ is the antiferromagnetic second-neighbour coupling.

$J$ and $J_1$ along the $z$ and $x$ axes, respectively, and the second-neighbour coupling along the $z$ axis is labelled $J_2$. In this study we shall take $J_1 = J$ although the method can easily be extended to include the anisotropic case. The model has been extensively studied in both two and three dimensions. In two dimensions both Monte Carlo computer simulations (Selke and Fisher 1980) and analytic studies (Villain and Bak 1981) show the presence of ferromagnetic, paramagnetic, incommensurate and $++--$

† Present address: Department of Mathematics, Imperial College of Science and Technology, London SW7 2BZ, UK.

0305-4470/87/020471+10$02.50  

(or $\langle 2 \rangle$) phases on varying the temperature and the ratio $J_2/J$. The $\langle 2 \rangle$ phase consists of a regular pattern of two rows of 'up' spins followed by two rows of 'down' spins along the $z$ direction in the lattice. Early Monte Carlo calculations (Selke and Fisher 1980) have predicted a multicritical point at non-zero temperature, but the phase diagram is now generally believed to be similar to that obtained by Villain and Bak (1981). Recently transfer matrix scaling techniques have been applied to the problem (Beale *et al* 1985). The phase diagram obtained is consistent with the result of Villain and Bak (1981).

In this paper we present numerical results for the 2D spin-$\frac{1}{2}$ ANNNI model. We use a new iterative method, the method of ring recurrence (McKenzie 1986). The method is quite general and allows the critical properties of a system with a classical Hamiltonian to be studied in terms of effective fields or partial partition functions which are defined recursively. The existence of a phase transition is related to the stability of the fixed point of the iteration. For Bethe graphs for which the method is trivially exact, we have studied the Ising model with competing interactions (Saqi and McKenzie 1986a) and the random bond Ising model (McKenzie and Saqi 1986). In two dimensions, the method produces a matrix recursion. An approximation must be introduced to obtain a finite iterative scheme. This approximation is entirely equivalent to the familiar device used in renormalisation group methods of thinning out the number of degrees of freedom at each iteration, while retaining the dominant terms. The application of the method of ring recurrence to the ANNNI model enables the use of only low-order matrices and allows a direct calculation of the wavevector in the incommensurate phase.

In the next section we briefly outline the method of ring recurrence and describe its application to the 2D ANNNI model. In § 3 we present the phase diagram that we obtain and in § 4 we study the incommensurate phase in more detail. Finally, we give a few concluding remarks.

## 2. The iterative method

We give here a brief outline of the method of ring recurrence (McKenzie 1986) and its application to the ANNNI model.

The model is formulated as a discrete physical system $(G, \Phi, U)$ (McKenzie 1981), where $G$ is a graph with vertex set $V(G)$, edge set $E(G)$ and graph metric $d(x, y)$, $x, y \in V(G)$, $\Phi$ is the state space and $U$ is the potential. In this study $G$ is the square lattice, $\Phi = \prod_{x \in V(G)} \phi_x$, $\phi_x = \{1, -1\}$ and $U$ is given by

$$U = \beta H \sum_{x \in V(G)} \sigma_x + \beta J \sum_{[x,y] \in E(G)} \sigma_x \sigma_y + \beta J' \sum_{A \in G} \sigma_x \sigma_y$$

where $A = \{x, y: x, y \in V(G), d_z(x, y) = 2\}$ where $d_z$ is the metric in the $z$ direction.

We divide the graph into rings $X_s^\alpha$ relative to some origin $\alpha \in V(G)$ so that (see figure 2)

$$X_s^\alpha = \{x: x \in V(G), \quad d(x, \alpha) = s, \quad s = 0, 1, 2, \ldots\}.$$

Clearly $\bigcup_{s \geq 0} X_s^\alpha = V(G)$ and $X_s^\alpha \wedge X_t^\alpha = \phi$.

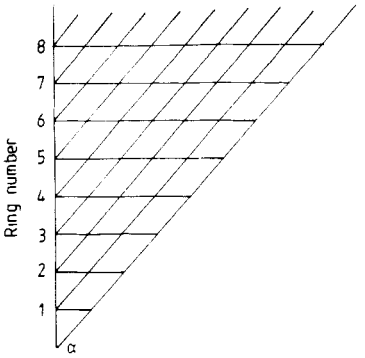


**Figure 2.** The 'wedge': $\alpha$ is the origin and rings are labelled as shown.

Let $\Omega_i = \Pi_{x \in X_i^a} \phi_x$ and consider $J(\omega_i, \omega_j, \omega_k, \omega_l)$ where $\omega_i \in \Omega_s$, $\omega_j \in \Omega_{s+1}$, $\omega_k \in \Omega_{s+2}$, $\omega_l \in \Omega_{s+3}$. We define

$$J(\omega_i, \omega_j, \omega_k, \omega_l) = \sum_{x \in X_{s+2}} j_x(\omega_k) + \sum_{x \in X_{s+3}} j_x(\omega_l) + \sum_{e \in E_{s+2}} j_e(\omega_k, \omega_k) + \sum_{e \in E_{s+3}} j_e(\omega_l, \omega_l)$$
$$+ \sum_{e \in E_{s+2,s+3}} j_e(\omega_k, \omega_l) + \sum_{e \in E_{s+1,s+2}} j_e(\omega_j, \omega_k)$$
$$+ \sum_{e \in E_{s+1,s+3}} j_f(\omega_j, \omega_l) + \sum_{e \in E_{s,s+2}} j_f(\omega_i, \omega_k).$$

$j_x$ are contributions to $U$ from each site or vertex, $j_e$ are contributions from each nearest-neighbour bond, $j_f$ are contributions from each second-nearest-neighbour bond and

$$E_{s+2} = \{[x, y];\ x, y \in X_{s+2};\ d(x, y) = 1\}$$
$$E_{s+2,s+3} = \{[x, y];\ x \in X_{s+2},\ y \in X_{s+3};\ d(x, y) = 1\}$$
$$E_{s,s+2} = \{[x, y];\ x \in X_s,\ y \in X_{s+2};\ d_2(x, y) = 2\}$$

with similar expressions for the other terms, $d_z$ being the metric in the $z$ direction.

In terms of $J$, the partition function of a finite graph $G_n$, for which $V(G_n) = \bigcup_{s \geq 0} X_s$, can be written as

$$Z_{G_n} = \sum \exp(J_\alpha(\omega_0)) \Big( \sum \exp(J(\omega_0, \omega_1, \omega_2)) \Big( \sum \exp(J(\omega_1, \omega_2, \omega_3, \omega_4))$$
$$\times \Big( \ldots \Big( \sum \exp(J(\omega_{n-3}, \omega_{n-2}, \omega_{n-1}, \omega_n)) \Big) \ldots \Big) \Big) \Big).$$

We define normalised effective fields $\mu_{s+1}(\omega_s, \omega_{s+1})$ recursively by

$$\gamma_{s+1} \mu_{s+1}(\omega_s, \omega_{s+1}) = \sum \exp(J(\omega_s, \omega_{s+1}, \omega_{s+2}, \omega_{s+3})) \mu_{s+3}(\omega_{s+2}, \omega_{s+3}) \tag{2.1}$$

where $\gamma$ is a suitable norm. The $\mu_{s+1}$ is a partial partition function which gives the contribution to $Z$ from that portion of the graph located further than $s+1$ rings from the origin $\alpha$.

We compare (2.1) with the corresponding expression for the simple Ising model with nearest-neighbour interactions only, namely

$$\gamma_{s+1}\mu_{s+1}(\omega_{s+1}) = \sum \exp(J(\omega_{s+1}, \omega_{s+2}))\mu_{s+2}(\omega_{s+2}).$$

We now particularise the general treatment given so far to the square lattice. It is easiest to develop the formalism for the graph shown in figure 2. In the thermodynamic limit the effects of the edges become negligible compared with the bulk terms. Our development concentrates on the bulk terms which is clearly equivalent to studying the square lattice.

The effective fields $\mu_{s+1}$ for this graph can be expressed as a product of matrices. Thus

$$\mu_{s+1}(\omega_s\omega_{s+1}) = K_{s+1}(\sigma_{s,1}, \sigma_{s+1,1}) \prod_i A_{s+1}(\sigma_{s,i}, \sigma_{s+1,i})\mathbf{1}. \tag{2.2}$$

The first subscript on the spin variables $\sigma$ labels the ring and the second subscript labels the position of a spin along a ring.

Similarly, $\mu_{s-1}$ is given by

$$\mu_{s-1}(\omega_{s-2}, \omega_{s-1}) = K_{s-1}(\sigma_{s-2,1}, \sigma_{s-1,1}) \prod_i A_{s-1}(\sigma_{s-2,i}, \sigma_{s-1,i})\mathbf{1}. \tag{2.3}$$

There is a matrix recursion between the $A_{s+1}$ and the $A_{s-1}$. The $K$ matrices are edge terms and are later neglected.

For the spin-$\frac{1}{2}$ Ising model with nearest-neighbour interactions, the matrix recursion is (McKenzie 1986)

$$\gamma_{s-1}A_{s-1}(\sigma) = \begin{pmatrix} x(\sigma)\,e^{J}A_s(1) & x^{-1}(\sigma)\,e^{-J}A_s(-1) \\ x(\sigma)\,e^{-J}A_s(1) & x^{-1}(\sigma)\,e^{J}A_s(-1) \end{pmatrix} \tag{2.4}$$

where $x(\sigma) = \exp(H + \sigma J)$, $x^{-1}(\sigma) = \exp(-H - \sigma J)$ and $\gamma$ is a norm.

Up to this stage the formalism is exact. To obtain a recurrence scheme the matrix recursion is reduced to a recursion between scalars. The matrices $A_s(\sigma_{s,i})$ are diagonalised and contributions to the product $\Pi\, A_s(\sigma_{s,i})$ involving only the largest eigenvalues are retained.

The matrix recursion (2.4) for the simple spin-$\frac{1}{2}$ Ising model becomes, in this approximation,

$$\gamma_{s-1}A_{s-1}(\sigma) = \begin{pmatrix} x(\sigma)\,e^{J} & x^{-1}(\sigma)\,e^{-J}\mu a_{11}(1,-1) \\ x(\sigma)\,e^{-J}a_{11}(-1,1) & x^{-1}(\sigma)\,e^{J}\mu \end{pmatrix} \tag{2.5}$$

where $\mu = \lambda_1(-1)/\lambda_1(1)$ and $\lambda_1(\sigma)$ is the largest eigenvalue of the matrix $A(\sigma)$; $a_{11}(\sigma_1, \sigma_j)$ is the (1, 1) element of the matrix product $T^{-1}(\sigma_i)T(\sigma_{i+1})$, where $T^{-1}AT = \Lambda$, the matrix of eigenvalues, $\gamma$ is a suitable norm.

The recursion relation (2.5) is studied numerically by computing the matrices $A(\sigma)$ and their eigenvalues and eigenvectors for arbitrary initial values of $\lambda_1(\sigma)$ and $a_{11}(\sigma_i, \sigma_{i+1})$. The critical point $T_c$ is obtained from the behaviour of the fixed point $\mu^*$. For $T > T_c$, $\mu^* = 1$, whilst for $T < T_c$, $\mu^* = 1$ becomes unstable and the solution bifurcates at $T = T_c$.

For the ANNNI model the inclusion of the axial second-nearest-neighbour coupling groups the spins into pairs and forces us to consider the problem as a four-state model. A pair of spins $(\sigma_{s,i}, \sigma_{s+1,i})$ can be in one of the four possible states, namely $++$, $+-$, $-+$, $--$ and similarly for the adjacent pair $(\sigma_{s,i+1}, \sigma_{s+1,i+1})$. We label the four states

by $\tau$ which takes values 1, 2, 3, 4. We define

$$b_{mn} = a_{11}(\tau_i = m, \tau_{i+1} = n) \qquad m, n = 1, 2, 3, 4$$

where $a_{11}$ is the leading diagonal element of $T^{-1}(\tau_i)T(\tau_{i+1})$ where $T^{-1}AT = \Lambda$.

Here $\tau_i$ refers to the pair of spins $(\sigma_{s+1,i}, \sigma_{s,i})$ and $\tau_{i+1}$ refers to $(\sigma_{s+1,i+1}, \sigma_{s,i+1})$ (refer to figure 3).

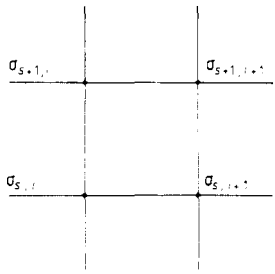

**Figure 3.** Refer to text.

Following the method of ring recurrence (McKenzie 1986) we reduce the matrix recursion defined by (2.2) and (2.3) to a recursion between scalars. The matrix recursion is

$$\gamma_{s-1}A_{s-1}(\sigma_i, \sigma_j) = \begin{pmatrix} t_1A_{s+1}(1,1)\,e^{3J} & t_2A_{s+1}(1,-1)\,e^{-J} & t_3A_{s+1}(-1,1)\,e^{-J} & t_4A_{s+1}(-1,-1)\,e^{-J} \\ t_1A_{s+1}(1,1)\,e^{J} & t_2A_{s+1}(1,-1)\,e^{J} & t_3A_{s+1}(-1,1)\,e^{-3J} & t_4A_{s+1}(-1,-1)\,e^{J} \\ t_1A_{s+1}(1,1)\,e^{J} & t_2A_{s+1}(1,-1)\,e^{-3J} & t_3A_{s+1}(-1,1)\,e^{J} & t_4A_{s+1}(-1,-1)\,e^{J} \\ t_1A_{s+1}(1,1)\,e^{J} & t_2A_{s+1}(1,-1)\,e^{-J} & t_3A_{s+1}(-1,1)\,e^{-J} & t_4A_{s+1}(-1,-1)\,e^{3J} \end{pmatrix}$$

where $\sigma_i \in \Omega_s$, $\sigma_j \in \Omega_{s+1}$ and

$$t_1(\sigma_i, \sigma_j) = \exp[2H + \sigma_i(J_2 + J) + \sigma_jJ_2]$$

$$t_2(\sigma_i, \sigma_j) = \exp[\sigma_i(J_2 - J) - \sigma_jJ_2]$$

$$t_3(\sigma_i, \sigma_j) = \exp[\sigma_i(J - J_2) + \sigma_jJ_2]$$

$$t_4(\sigma_i, \sigma_j) = \exp[-2H - \sigma_i(J_2 + J) - \sigma_jJ_2].$$

We obtain

$$\gamma_{s+1}A_{s+1}(\sigma_i, \sigma_j) = \begin{pmatrix} t_1\,e^{3J}\lambda_1(1,1)b_{11} & t_2\,e^{-J}\lambda_1(1,-1)b_{12} & t_3\,e^{-J}\lambda_1(-1,1)b_{13} & t_4\,e^{-J}\lambda_1(-1,-1)b_{14} \\ t_1\,e^{J}\lambda_1(1,1)b_{21} & t_2\,e^{J}\lambda_1(1,-1)b_{22} & t_3\,e^{-3J}\lambda_1(-1,1)b_{23} & t_4\,e^{J}\lambda_1(-1,-1)b_{24} \\ t_1\,e^{J}\lambda_1(1,1)b_{31} & t_2\,e^{-3J}\lambda_1(1,-1)b_{32} & t_3\,e^{J}\lambda_1(-1,1)b_{33} & t_4\,e^{J}\lambda_1(-1,-1)b_{34} \\ t_1\,e^{J}\lambda_1(1,1)b_{41} & t_2\,e^{-J}\lambda_1(1,-1)b_{42} & t_3\,e^{-J}\lambda_1(-1,1)b_{43} & t_4\,e^{3J}\lambda_1(-1,-1)b_{44} \end{pmatrix}.$$

We normalise $A_{s+1}$ by letting $\gamma_{s+1} = \lambda_1^{(s+1)}(1)$.

We now have a recursion relation between scalar quantities. We shall examine the behaviour of the eigenvalues of $\boldsymbol{A}$ upon iteration. Each eigenvalue is associated with one of the four combinations of a pair of spins $(\sigma_i, \sigma_j)$. The terms $b_{mn}$ represent the weight attached to transforming the configuration of a given spin pair $n$ into the configuration $m$ of the adjacent spin pair under the operation of the matrix $\boldsymbol{A}$.

### 3. The phase diagram

The various phases are characterised by the behaviour of the eigenvalues on iteration. We obtain four distinct phases.

(a) A paramagnetic phase where the eigenvalues iterate to fixed points $\lambda^*$, such that

$$\lambda_1^*(1) = \lambda_1^*(4) \qquad \text{and} \qquad \lambda_1^*(2) = \lambda_1^*(3).$$

We find that at the fixed point

$$b_{mn} = b_{m'n'}$$

if we write $m'$ as the complementary state to $m$, so that $\tau(m') = \tau(-\sigma_i - \sigma_j)$, when $\tau(m) = \tau(\sigma_i, \sigma_j)$. This is the expected behaviour since in the paramagnetic phase it is equally likely for a given spin to be up or down. Thus, in this phase, the matrix $\boldsymbol{A}$ becomes symmetrical. The appearance of ferromagnetism is therefore a consequence of symmetry breaking.

(b) The ferromagnetic phase: here the fixed points are such that

$$\lambda_1^*(1) \neq \lambda_1^*(2) \neq \lambda_1^*(3) \neq \lambda_1^*(4).$$

On iteration the $b_{mn}$ converge to fixed points such that

$$b_{13} = b_{14} = b_{23} = b_{24} = 0$$

$$b_{31} = b_{32} = b_{41} = b_{42} = 0.$$

In other words, the $b_{mn}$ in the diagonal $(2 \times 2)$ blocks converge to zero.

(c) The $++--$ or $\langle 2 \rangle$ phase: the eigenvalues $\lambda_1^*(\tau)$ iterate to a 2-cycle. There are two stable fixed points between which the system alternates in a stable cycle of period two. Each step in the iteration takes into account two rows (or rings) of the lattice. In terms of the actual lattice, the 2-cycle observed is a $++--$ phase with two rows having 'up' spins and two rows having 'down' spins in a regular manner. In this phase we find the $b_{mn}$ iterate to fixed points, $b_{mn} = 0$, $m \neq n$. For $m = n$, $b_{mm} \equiv 1$. This behaviour of the $b_{mn}$ is consistent with a $++--$ structure. For such a structure we would not expect a change of sign going along a row and hence the expected weights of such configurations would be zero.

(d) Finally we observe regions where the eigenvalues do not converge but take on an oscillatory chaotic-like behaviour. This characterises the incommensurate phase. In this region we detect no regular behaviour of the $b_{mn}$.

The phase diagram is shown in figure 4. We note the phase boundary between the incommensurate and paramagnetic phases moves slightly to the left of the line $-J_2/J = 0.5$, before returning to $-J_2/J = 0.5$ as $T$ decreases. This effect, though small, is certainly present. Detailed numerical studies show there is no multicritical point at a non-zero temperature where the three phases—ferromagnetic, paramagnetic and incommensurate—meet. The paramagnetic phase extends down to $T = 0$ (figure 5). Apart from this our phase diagram is similar to that obtained by Villain and Bak (1981) and Beale *et al* (1985).

In figure 6 we compare our numerical results for the paramagnetic-ferromagnetic phase boundary with the curve predicted by Hornreich *et al* (1979), who determine $T_c$ by the vanishing of an interface free energy.

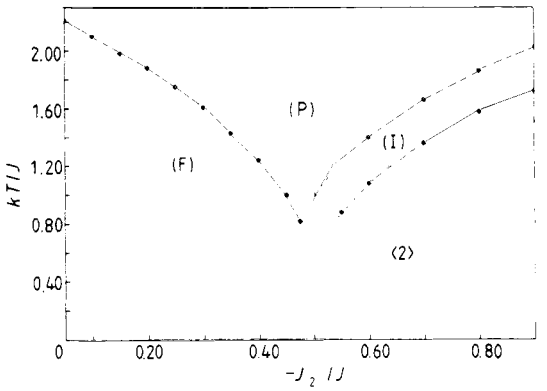


**Figure 4.** Phase diagram for spin-$\frac{1}{2}$ 2D ANNNI model. (P) = paramagnetic, (F) = ferromagnetic, (I) = incommensurate, $\langle 2 \rangle = ++--$ phase.

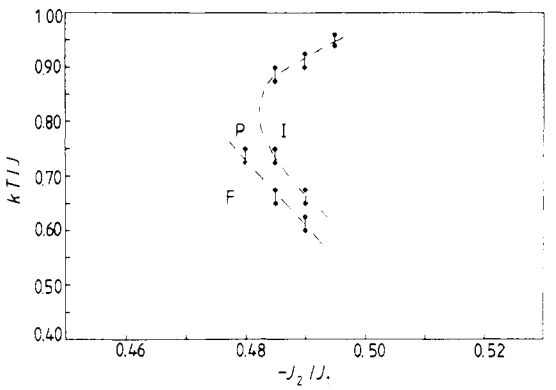


**Figure 5.** Detailed study of the phase diagram close to $-J_2/J = 0.5$.

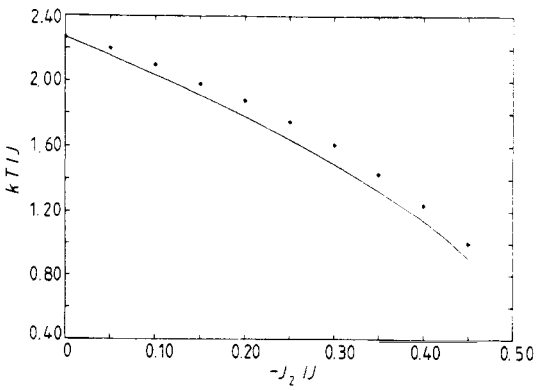


**Figure 6.** Ferromagnetic-paramagnetic phase boundary: the points are our numerical results; the curve is from Hornreich *et al* (1979).

## 4. The incommensurate phase

We now study further the incommensurate phase. Our iterative scheme enables us to obtain a direct estimate of the wavevector. Each iteration corresponds to moving spatially through two rings of the lattice and the fixed point describes the bulk behaviour.

Following Vannimenus (1981) we define two order parameters:

$$\eta_1 = [\lambda_1(1) - \lambda_1(4)]/[\lambda_1(1) + \lambda_1(4)]$$

$$\eta_2 = [\lambda_1(2) - \lambda_1(3)]/[\lambda_1(1) + \lambda_1(4)].$$

Clearly $\eta_1$, $\eta_2$ converge to zero in the paramagnetic phase and to non-zero fixed points in the ferromagnetic phase. We define the wavevector by

$$q = \lim_{N\to\infty} n(N)/4N \tag{4.1}$$

where $n(N)$ is the number of times the order parameter changes sign in $N$ iterations. We have divided by 4 due to the fact that on each iteration we move through two rings of the lattice.

Figure 7 shows a plot of $\eta_1$ against $\eta_2$ at a typical point in the incommensurate phase ($J^{-1} = kT/j = 1.4$, $-J_2/J = 0.7$). We observe that this phase is characterised by the existence of a one-dimensional attractor. The corresponding power spectrum is shown in figure 8.

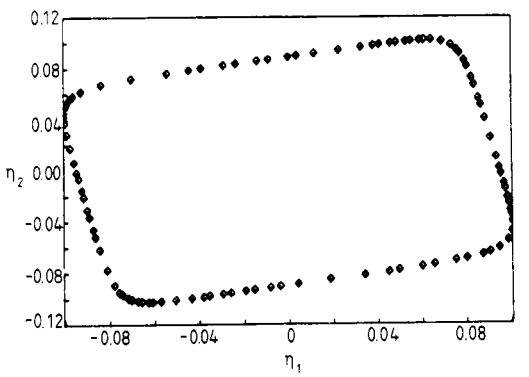


**Figure 7.** Attractor in (I) phase ($J^{-1} = 1.4$, $-J_2/J = 0.7$).

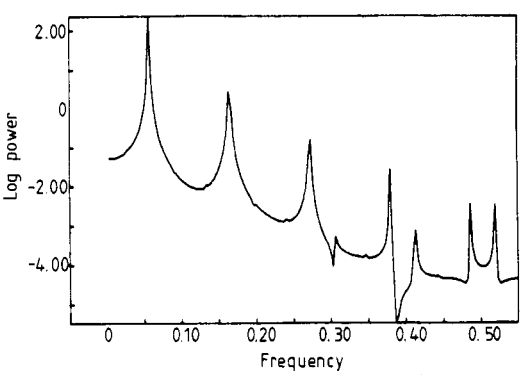


**Figure 8.** Power spectrum corresponding to figure 7.

The variation of the wavevector, $q$, with temperature for two values of competing interaction strength $-J_2/J = 0.7$, $-J_2/J = 0.9$ is given in figures 9 and 10. The definition (4.1), whilst very convenient for numerical purposes, requires a large number of iterations, $N$. For Bethe graph models (Saqi and McKenzie 1986a) the recursive scheme yields a simple set of coupled non-linear equations, and it is easy to take $N$ to be the order of 10 000. In the present case, however, due to CPU time limitations we have taken $N = 650$ in obtaining the results shown in figures 9 and 10. There is evidence of frequency locking in the figures. More detailed calculations suggest that frequency locking is a persistent feature of the behaviour of this model in the incommensurate phase.

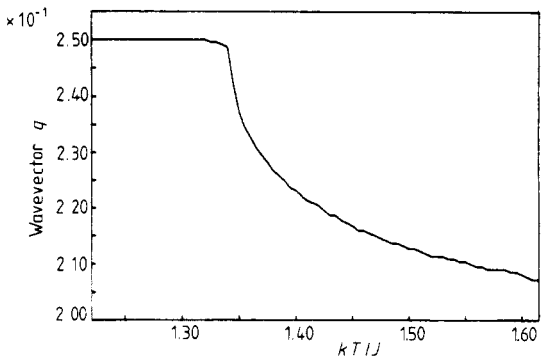


**Figure 9.** Variation of wavevector with temperature $(-J_2/J = 0.7)$.

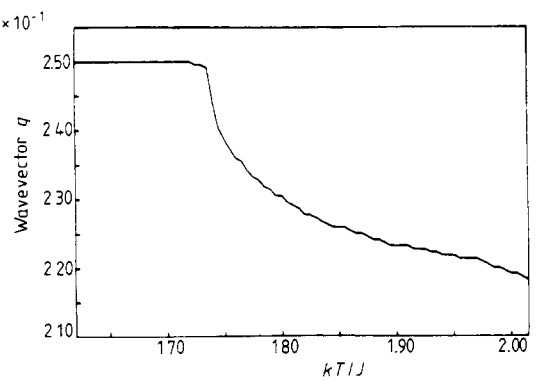


**Figure 10.** Variation of wavevector with temperature $(-J_2/J = 0.9)$.

## 5. Conclusions

We have studied the 2D ANNNI model using a new iterative method, the method of ring recurrence (McKenzie 1986). Within the approximation of the two-dimensional formulation we are able to obtain rather accurate estimates of the phase boundaries or critical frontiers. The phase diagram is in general agreement with other results (Villain and Bak 1981, Beale *et al* 1985). We note however the existence of the

incommensurate phase for $-J_2/J < 0.5$. There is no evidence for the existence of a multicritical point on the ferromagnetic phase boundary, at the position predicted by Selke and Fisher (1980). Rather, from the evidence of figures 4 and 5, we suggest that the paramagnetic phase reaches $T = 0$. We have found that the incommensurate phase is associated with a one-dimensional attractor as in the case of incommensurate phases on Bethe lattice models with competing second-neighbour interactions (Inawashiro *et al* 1983). Our formulation allows us to obtain a direct estimate of the wavevector, $q$, which is convenient for numerical purposes. The variation of $q$ with temperature points strongly to frequency locking over small temperature intervals. Our feeling is that frequency locking is a real effect of the model, as in Bethe lattice models, and is not caused by the finite number of iterations or the approximation made in the formulation of the method. The peaks and dips in the power spectrum show that the model predicts that the diffuse scattering from the incommensurate phase is not uniform.

We have explored the possibility of finding the disorder line (Stephenson 1970) but have not pursued this in depth. Preliminary studies show that the disorder line can be determined by the mode by which the order parameter converges to zero in the paramagnetic phase: to the left of the disorder line convergence is monotonic, to the right it is oscillatory. It is straightforward to test for this behaviour numerically and hence to obtain an indication of the position of the disorder line.

We have been somewhat surprised by how easily the method can be implemented on this fairly complex model and the accuracy with which the phase boundaries can be obtained with very modest expenditure of computer time. Finally, we observe that the method is easily generalised to higher spins. The spin-1 ANNNI model involves matrices of order nine and determination of the phase diagram is relatively straightforward (Saqi and McKenzie 1986b).

## References

Beale P, Duxbury P M and Yeomans J 1985 *Preprint* Oxford University
Elliot R J 1961 *Phys. Rev.* **124** 346
Hornreich R M, Liebmann R, Schuster H G and Selke W 1979 *Z. Phys.* B **35** 91
Inawashiro S, Thompson C J and Honda G 1983 *J. Stat. Phys.* **33** 419
McKenzie D S 1981 *J. Phys. A: Math. Gen.* **14** 3267
—— 1986 to be submitted
McKenzie D S and Saqi M A S 1986 *J. Phys. A: Math. Gen.* **19** 3883
Saqi M A S and McKenzie D S 1986a *J. Stat. Phys.* submitted
—— 1986b to be submitted
Selke W and Fisher M E 1980 *Z. Phys.* B **40** 71
Stephenson J 1970 *J. Math. Phys.* **11** 413
Vannimenus J 1981 *Z. Phys.* B **43** 141
Villain J and Bak P 1981 *J. Physique* **42** 657